ADVANCED ENERGY MATERIALS

Supporting Information

for *Adv. Energy Mater.,* DOI: 10.1002/aenm.202203174

Current-Dependent Lithium Metal Growth Modes in "Anode-Free" Solid-State Batteries at the Cu|LLZO Interface

Till Fuchs, Juri Becker, Catherine G. Haslam, Christian Lerch, Jeff Sakamoto, Felix H. Richter, and Jürgen Janek**

Current-Dependent Lithium Metal Growth Modes in 'Anode-Free' Solid-State-Batteries at the Cu|LLZO Interface

Till Fuchs[1,2,Δ], Juri Becker[1,2,Δ], Catherine G. Haslam[3,4], Christian Lerch,[1,2]
Jeff Sakamoto[3,4], Felix H. Richter[1,2*] and Jürgen Janek[1,2*]

[1]Institute of Physical Chemistry, Justus-Liebig-University Giessen, Heinrich-Buff-Ring 17, D-35392 Giessen, Germany.

[2]Center for Materials Research (ZfM), Justus-Liebig-University Giessen, Heinrich-Buff-Ring 16, D-35392 Giessen, Germany.

[3]Department of Materials Science and Engineering, University of Michigan, Ann Arbor, MI 48109, USA

[4]Department of Mechanical Engineering, University of Michigan, Ann Arbor, MI 48109, USA

[Δ] denotes equal contributions

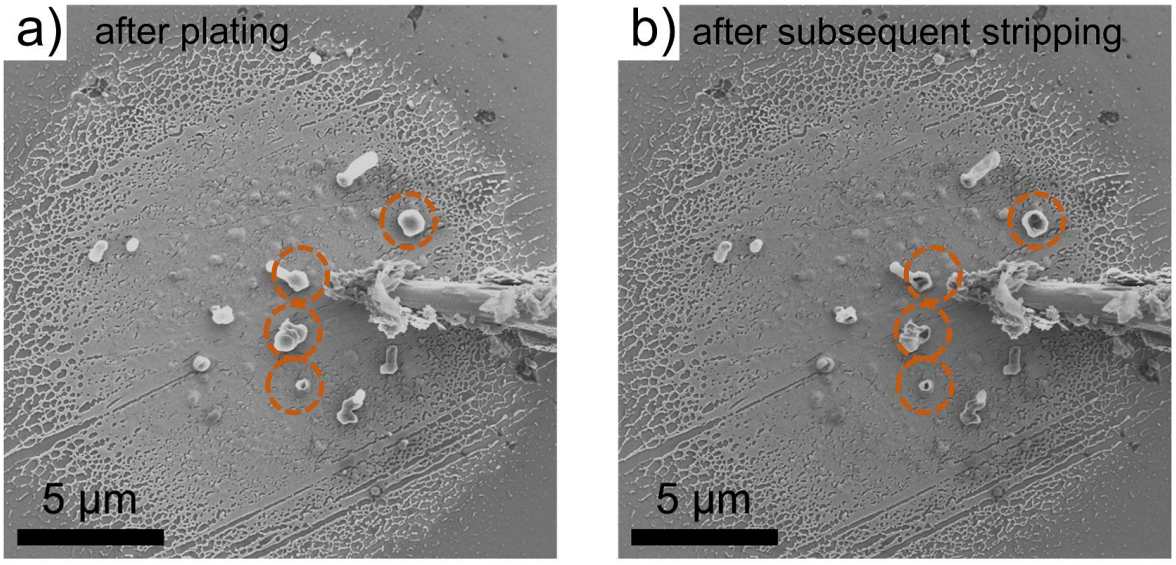

Figure S1. The lithium morphology after plating with 50 µA cm^{-2} is shown on the left in a). During stripping, a fast contact loss and increase in overvoltage is reached due to the low areal coverage of lithium. This is visible in the particles collapsing upon stripping, herein marked with orange circles. This resulted in a low coulombic efficiency of 13%.

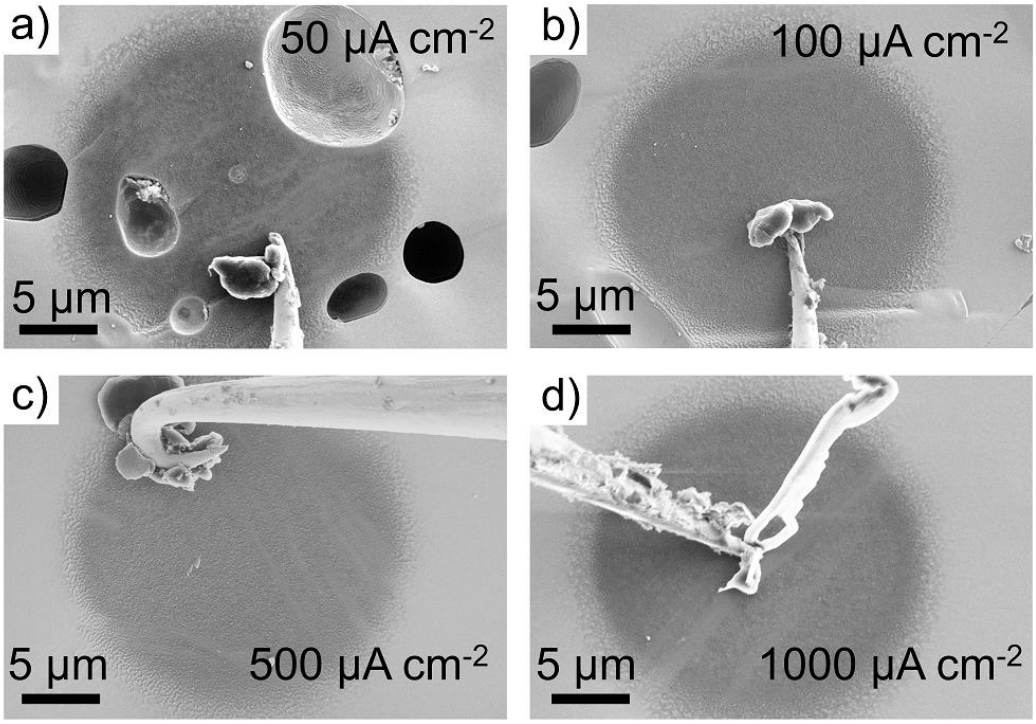

Figure S2. a) SEM micrographs depicting the lithium morphology after plating with 50 µA cm^{-2} at Cu|LLZO$_{sc}$ interfaces. The single-crystalline LLZO surface was achieved by controlling the LLZO grain size to be larger than the copper current collector patch. Morphologies after plating with 100 µA cm^{-2}, 500 µA cm^{-2} and 1000 µA cm^{-2} are depicted in b), c) and d), respectively.

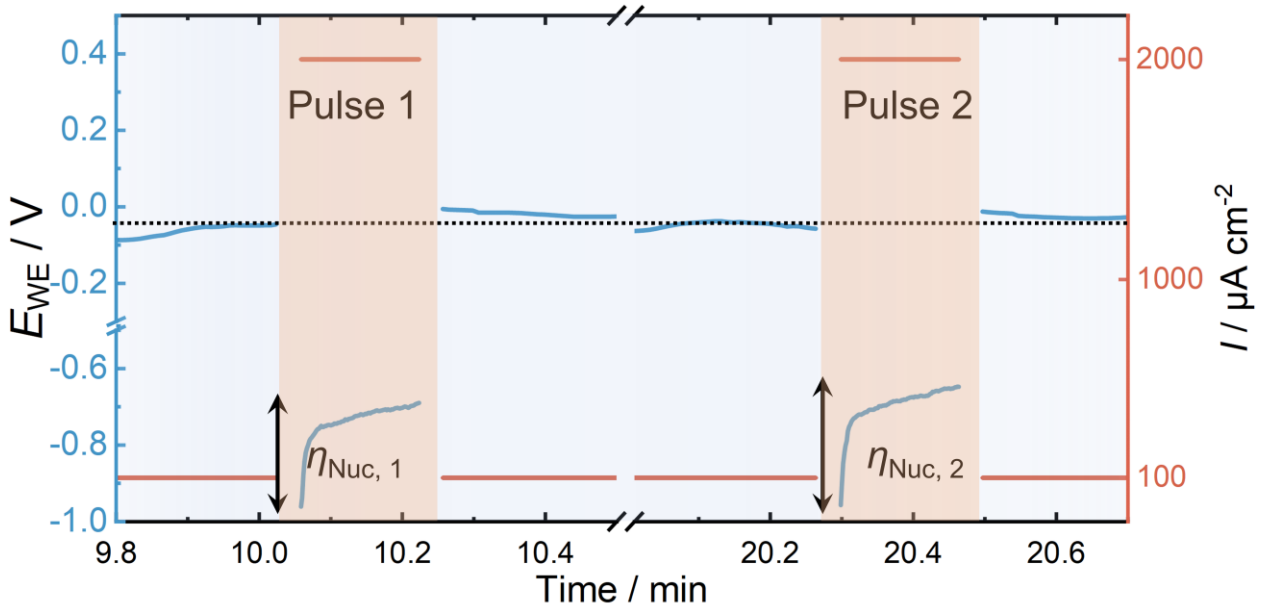

Figure S3. Magnified plot of the current pulses during the plating experiment. The overvoltage shows that lithium nucleates at new spots despite growth happening already at other areas within the sample.

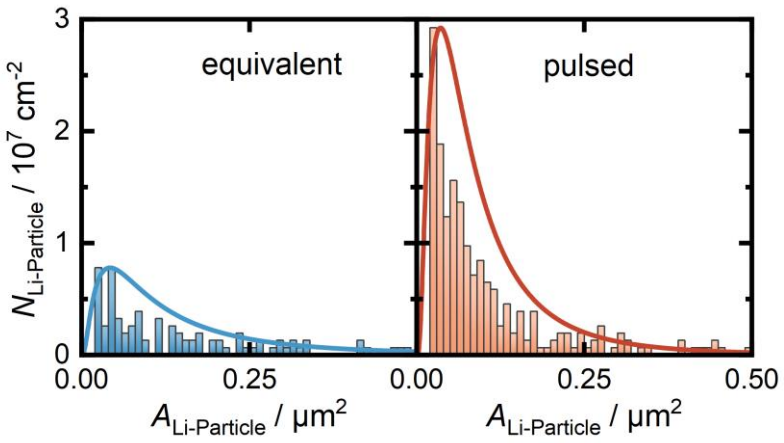

Figure S4. Histogram of the particle size distribution after plating continuously with 100 µA cm^{-2} (left) and after using a pulsed "advanced charging" (right). A clear increase in the number of smaller particles is evident.

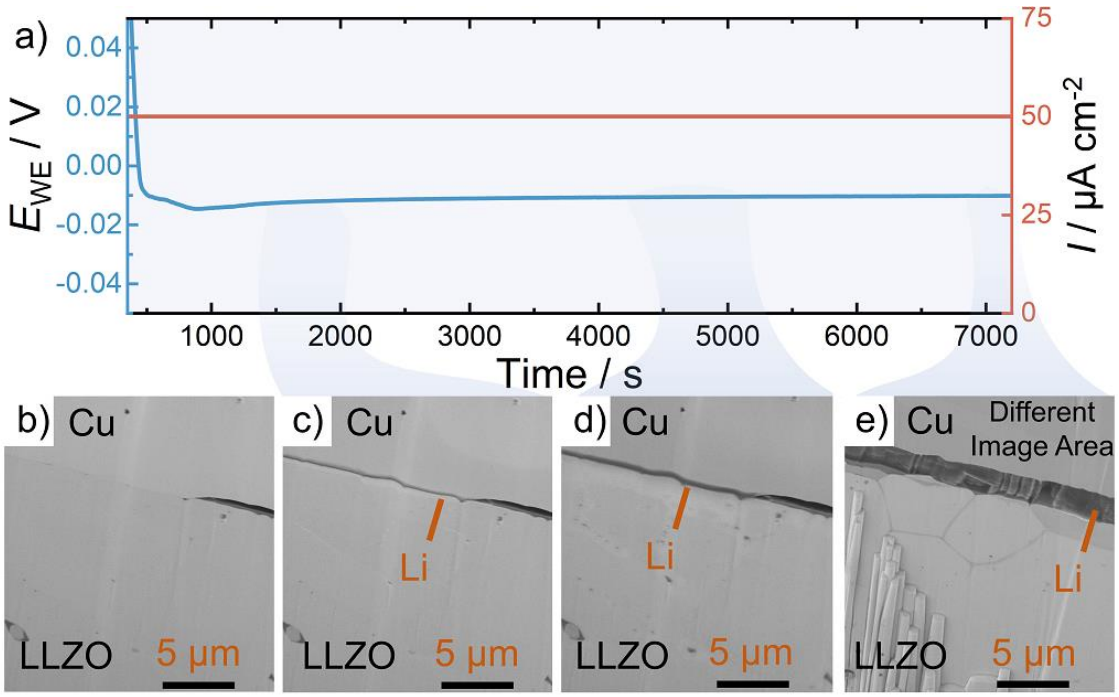

Figure S5. a) Voltage profile of lithium deposition observed at a Cu_{foil}|LLZO cross-section with 50 µA cm^{-2} applied. Respective SEM images during the process are depicted in b) – e). Note that e) shows a different image area than the other SEM images. Grain boundaries are visible after prolonged observation times due to electron beam induced lithium plating. Similar to the growth process with 100 µA cm^{-2}, a mix between whisker (mode (1)) and layer growth (mode (2)) is observed without any indication of lithium filament/dendrite growth. Additionally, the thickness of grown lithium is not perfectly homogeneous over the whole cross-section.

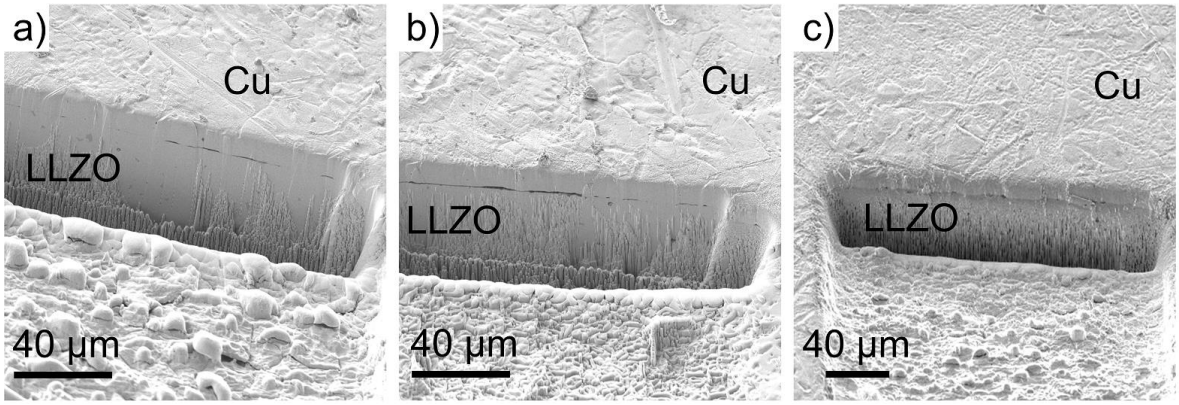

Figure S6. Low-magnification images of the cross-sections used for plating with 50 µA cm^{-2} (a), 100 µA cm^{-2} (b) and 500 µA cm^{-2} (c). Note that due to the tilted sample geometry, the error bar is not scaled perfectly.

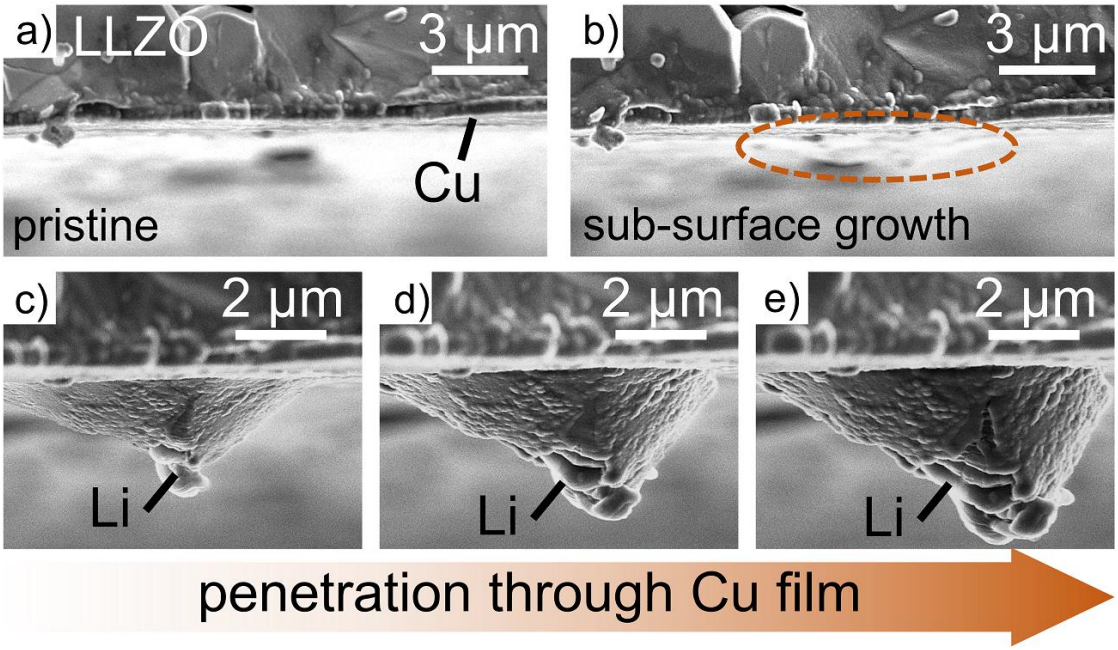

Figure S7. a) Cross-sectional overview over the herein investigated LLZO|Cu$_{film,400nm}$ electrode system. A film thickness of 400 nm was chosen to obtain a better cross-sectional visibility for the SEM experiment. We believe that the gained qualitative insight can be transferred to thinner films. At the beginning of the plating, sub-surface growth is visible in b), which then breaks through the copper layer as magnified at different stages in c), d) and e).

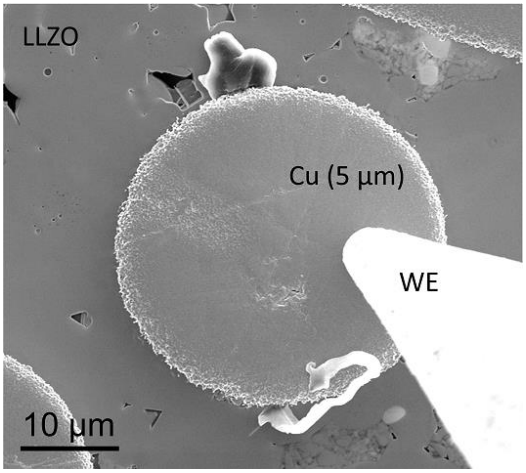

Figure S8: SEM micrograph of lithium being plated at thick $Cu_{5\mu m}$ films deposited on LLZO. Only at the edges of the prepared Cu patch, lithium is visibly growing, which only occurs due to the small size of the electrode. While this setup is unsuitable for characterizing the lithium growth as a function of the current density, it shows that the thicker Cu film is mechanically more stable and suppresses the penetration of growing lithium whiskers and particles through the current collector when compared to thin films used as shown in Figure 2.

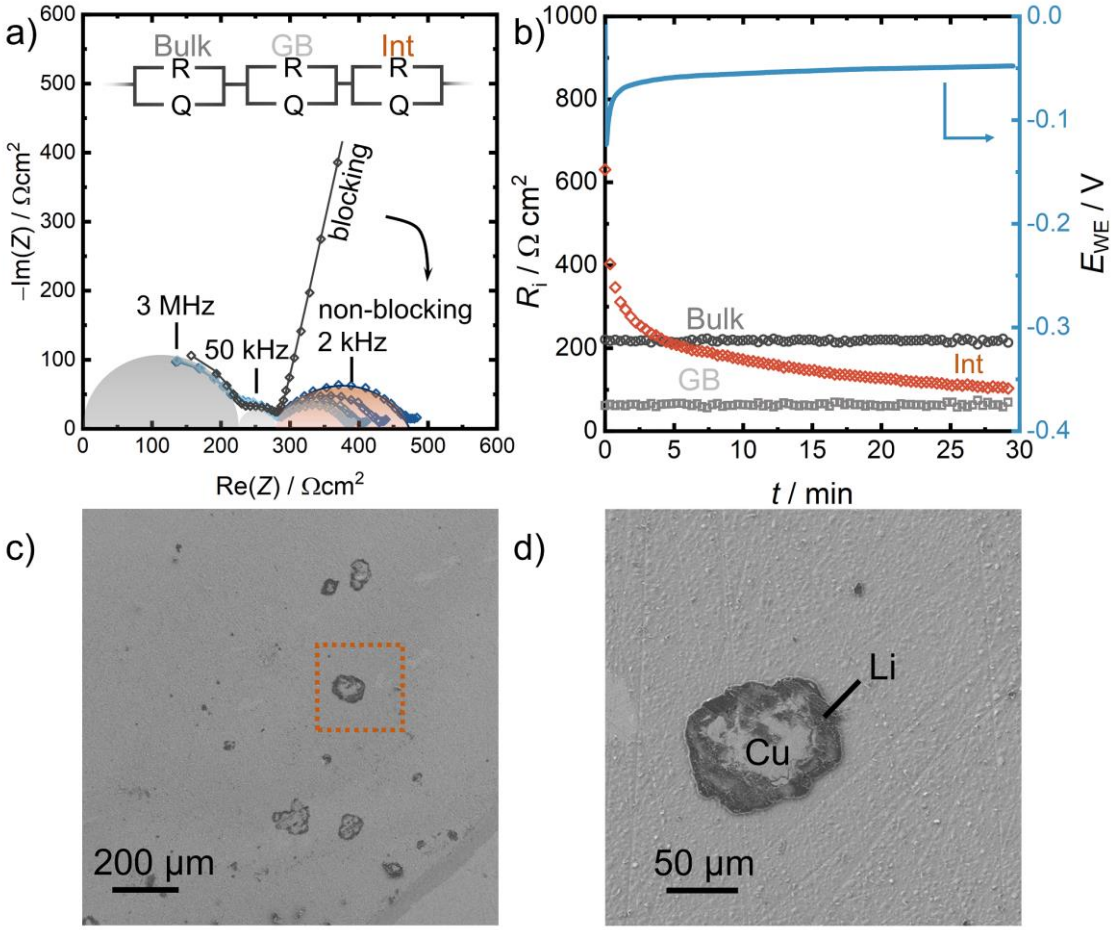

Figure S9. a) Impedance evolution when plating lithium at a Cu_{film}|LLZO interface with 100 µA cm^{-2} and 2 MPa of pressure applied. A clear transition between blocking and non-blocking impedance is observed once lithium has been deposited. Also, the good resolution and well separated

contributions of bulk and GB transport even before lithium plating indicate a conformal contact between Cu_{film} and LLZO. The extracted values of the three impedance contributions from a fit with the equivalent circuit in a) are depicted as a function of time in b) together with the voltage profile. SEM micrographs after plating are additionally shown in low (c) and high (d) magnification. Two different morphologies of grown lithium are visible. Below the thin Cu film, there is a large number of lithium particles in the size of around 1 µm present. The second observed lithium growth mode is that of a deformed whisker, which is in the size range of several tens of µm. Due to the small copper patch on top of the whisker, we conclude that once lithium penetrated the current collector film, it was plastically deformed and deposited above the rest of the CC. This is detrimental to the cell's performance, as no new contact area between lithium and LLZO is generated thereby.